J Appl Physiol 97: 874–882, 2004.
First published April 30, 2004; 10.1152/japplphysiol.01297.2003.

Probing the impact of axial diffusion on nitric oxide exchange dynamics with heliox

Hye-Won Shin,[1] Peter Condorelli,[1,2] Christine M. Rose-Gottron,[4] Dan M. Cooper,[3,4] and Steven C. George[1,2]

Departments of [1]Biomedical Engineering, [2]Chemical Engineering and Materials Science, and [3]Pediatrics, and [4]The General Clinical Research Center, University of California, Irvine, California 92697

Submitted 3 December 2003; accepted in final form 22 April 2004

Shin, Hye-Won, Peter Condorelli, Christine M. Rose-Gottron, Dan M. Cooper, and Steven C. George. Probing the impact of axial diffusion on nitric oxide exchange dynamics with heliox. *J Appl Physiol* 97: 874–882, 2004. First published April 30, 2004; 10.1152/japplphysiol.01297.2003.—Exhaled nitric oxide (NO) is a potential noninvasive index of lung inflammation and is thought to arise from the alveolar and airway regions of the lungs. A two-compartment model has been used to describe NO exchange; however, the model neglects axial diffusion of NO in the gas phase, and recent theoretical studies suggest that this may introduce significant error. We used heliox (80% helium, 20% oxygen) as the insufflating gas to probe the impact of axial diffusion (molecular diffusivity of NO is increased 2.3-fold relative to air) in healthy adults (21–38 yr old, $n = 9$). Heliox decreased the plateau concentration of exhaled NO by 45% (exhalation flow rate of 50 ml/s). In addition, the total mass of NO exhaled in phase I and II after a 20-s breath hold was reduced by 36%. A single-path trumpet model that considers axial diffusion predicts a 50% increase in the maximum airway flux of NO and a near-zero alveolar concentration ($C_{A_{NO}}$) and source. Furthermore, when NO elimination is plotted vs. constant exhalation flow rate (range 50–500 ml/s), the slope has been previously interpreted as a nonzero $C_{A_{NO}}$ (range 1–5 ppb); however, the trumpet model predicts a positive slope of 0.4–2.1 ppb despite a zero $C_{A_{NO}}$ because of a diminishing impact of axial diffusion as flow rate increases. We conclude that axial diffusion leads to a significant backdiffusion of NO from the airways to the alveolar region that significantly impacts the partitioning of airway and alveolar contributions to exhaled NO.

gas exchange; model; exhaled breath

NITRIC OXIDE (NO) performs many important functions in the lungs and has been regarded as a potential noninvasive marker of lung inflammation (2). The characteristics of NO gas exchange are unique compared with other endogenous gases because exhaled NO is thought to have a significant alveolar and airway source (6, 8, 15, 22). A two-compartment model is commonly used to characterize NO exchange dynamics for healthy and diseased lungs (9, 11, 13, 20, 21, 23, 24, 27, 29), by partitioning exhaled NO into airway and alveolar contributions using three flow-independent NO exchange parameters: maximum flux of NO from the airways ($J'aw_{NO}$), the diffusing capacity of NO in the airways (Daw_{NO}), and the steady-state alveolar concentration ($C_{A_{NO}}$). However, the two-compartment model considers only convection of NO in the airways as a transport mechanism and has neglected axial diffusion of NO in the gas phase to preserve mathematical simplicity.

Recently, our laboratory (17) and others (31) separately demonstrated theoretically that axial diffusion may play an important role in NO transport. During exhalation, the concentration of NO is higher in the airways compared with the alveoli, creating a gradient for diffusion of NO from the airways to the alveolar region (the opposite direction of convection). Thus the alveolar region may serve as a sink for NO produced in the airways, and neglecting axial diffusion may introduce significant error in the estimation of the flow-independent NO parameters such as $J'aw_{NO}$ and $C_{A_{NO}}$. On the basis of our earlier theoretical result (17), we hypothesize that axial diffusion of NO in the gas phase significantly reduces exhaled NO concentration by "backdiffusion" of NO from the airways to the alveolar region. The backdiffusion of NO may falsely lower the estimate of airway flux (i.e., $J'aw_{NO}$) and elevate the steady-state alveolar concentration (i.e., $C_{A_{NO}}$).

To probe the impact of axial diffusion experimentally, the present study utilized heliox as the insufflating gas during a single-breath maneuver. Heliox is a mixture of 80% helium and 20% oxygen that increases the molecular diffusivity of NO 2.3-fold in the gas phase relative to air while introducing only a minimal impact on upper airway gas mixing because of a lower density (See METHODS and DISCUSSION for details). We found that heliox decreased the concentration of NO in the exhaled breath during all three phases of the exhalation profile. Analysis of the data by a single-path trumpet model that considers axial diffusion suggests that backdiffusion of NO from the airways to the alveolar region significantly impacts the partitioning of exhaled NO into airway and alveolar contributions.

Glossary

$A_{I,II}$	Total mass of NO exhaled in phase I and II, which is defined by the area under the curve in phase I and II of the exhaled NO profile (ppb·ml)
$\hat{A}_{I,II}$	Experimentally determined mass of NO exhaled in phase I and II of the composite experimental profile, which serves as the "gold standard" for theoretical simulations (ppb·ml)
$A^*_{I,II}$	Model-predicted mass of NO exhaled in phase I and II of the composite experimental profile which serves as the gold standard for theoretical simulations (ppb·ml)

Address for reprint requests and other correspondence: S. C. George, Dept. of Chemical Engineering and Materials Science, 916 Engineering Tower, University of California, Irvine, CA 92697-2575 (E-mail: scgeorge@uci.edu).

The costs of publication of this article were defrayed in part by the payment of page charges. The article must therefore be hereby marked "*advertisement*" in accordance with 18 U.S.C. Section 1734 solely to indicate this fact.

 8750-7587/04 $5.00 Copyright © 2004 the American Physiological Society

$A_{c,aw}(z)$ Cross-sectional area of airway space (cm^2)
$A_{c,A}(z)$ Cross-sectional area of alveolar space (cm^2)
C_{NO} Concentration (ppb) of NO in the gas phase of the lungs
C_{ANO} Mixed or average steady-state fractional concentration of NO in the gas phase of the alveolar region (ppb). A steady-state concentration is achieved for breath hold or exhalation times >10 s.
C_{ENO} Exhaled NO concentration (ppb)
$C_{ENO,\dot{V}E}$ Exhaled NO concentration at constant exhalation flow rate $\dot{V}_E$ (ppb)
C^*_{ENO} Model-predicted exhaled concentration (ppb)
$\hat{C}_{ENO}$ Experimentally measured exhaled concentration determined from the composite (or mean) exhalation profile from a group of healthy adults subjects. This parameter serves as the gold-standard for comparison to theoretical simulations (ppb).
C_{NOpeak} Maximum concentration of NO in phase I and II
Daw_{NO} Diffusing capacity (ml/s) of NO in the entire airway tree, which is expressed as the volume of NO per second per fractional concentration of NO in the gas phase [ml $NO\cdot s^{-1}\cdot$(ml NO/ml gas)$^{-1}$ or ml/s] and is equivalent to $pl\cdot s^{-1}\cdot ppb^{-1}$
Daw_{NO} Diffusing capacity of NO in the airway per unit axial distance ($ml\cdot s^{-1}\cdot cm^{-1}$)
D_{ANO} Diffusing capacity (ml/s) of NO in the alveoli, which is expressed as the volume of NO per second per fractional concentration of NO in the gas phase [ml $NO\cdot s^{-1}\cdot$(ml NO/ml gas)$^{-1}$] and is equivalent to $pl\cdot s^{-1}\cdot ppb^{-1}$
$\tilde{D}_{ANO}$ Diffusing capacity of NO in the alveoli per unit axial distance ($ml\cdot s^{-1}\cdot cm^{-1}$)
$D_{NO,air}$ Molecular diffusivity (diffusion coefficient) of NO in air (cm^2/s)
$D_{NO,heliox}$ Molecular diffusivity (diffusion coefficient) of NO in heliox (cm^2/s)
$J'aw_{NO}$ Maximum total volumetric flux ($ppb\cdot ml\cdot s^{-1}$ or pl/s) of NO from the airways equal to the product of Daw_{NO} and Caw_{NO}
$\tilde{J}'aw_{NO}$ Maximum total volumetric flux of NO from the airways per unit axial distance ($ppb\cdot ml\cdot s^{-1}\cdot cm^{-1}$)
J'_{ANO} Maximum total volumetric flux ($ppb\cdot ml\cdot s^{-1}$ or pl/s) of NO from the alveoli equal to the product of D_{ANO} and C_{ANO}
$\tilde{J}'_{ANO}$ Maximum total volumetric flux of NO from the alveoli per unit axial distance ($ppb\cdot ml\cdot s^{-1}\cdot cm^{-1}$)
$N(z)$ Number of alveoli per unit axial distance
N_t Total number of alveoli
N_{max} Maximum number of alveoli at any axial position
n_{III} Number of data points in phase III of the exhalation profile
R_{III} Root mean square error between experimental data and model prediction in phase III of the exhalation profile
V Axial (or longitudinal) position from the distal region of the airway to the mouth (cm)
$\dot{V}$ volumetric flow rate of air (ml/s)
$\dot{V}_E$ $\dot{V}$ during expiration (ml/s)
$\dot{V}_I$ $\dot{V}$ during inspiration (ml/s)
$\dot{V}_{NO}$ Elimination rate of NO during expiration (ml NO/s)
$V_{I,II}$ Exhaled volume in phase I and II of the exhalation profile (ml)
W_{50} width of the phase I and II peak calculated by taking the volume at which the exhaled concentration is larger than 50% of C_{NOpeak}
z Axial position in the lungs (cm)
$z = L$ Axial position at the end of the trumpet
$z = L^+$ A single node just beyond the end of the trumpet

METHODS

Experiment

Subjects. Nine healthy adults (five women) participated in this study, and their characteristics are presented in Table 1. All subjects had an forced expiratory volume in 1 s (FEV_1) to forced vital capacity (FVC) ratio > 0.80, and those with a history of smoking at any time, cardiovascular, pulmonary, or neurological diseases were excluded.

Table 1. *Physical characteristics of subjects*

Sub	Gen	Age, yr	Hgt, m	Wgt, kg	Iwgt, kg	V_{air}, ml	FVC		FEV_1		FEV_1/FVC	
							liters	%pred	liters	%pred	%	%pred
1	M	38	1.75	65.9	72.7	198	5.16	104	4.04	100	78	96
2	F	36	1.50	47.3	45.5	136	3.5	121	2.96	118	85	98
3	F	34	1.50	42.7	45.5	134	3.31	114	2.81	110	85	97
4	F	28	1.63	50.9	54.5	148	3.5	91	3.01	98	86	108
5	M	24	1.80	97.3	78.2	196	5.61	102	4.18	88	75	87
6	F	23	1.63	54.5	54.5	143	3.81	106	3.51	112	92	106
7	M	23	1.78	93.2	75.5	189	5.84	110	5.19	114	89	104
8	F	21	1.57	54.5	50.0	131	3.54	103	3.2	105	90	101
9	M	25	1.68	65.5	67.3	173	5.88	123	4.41	109	75	89
Mean		28.0	1.65	63.5	60.4	161	4.46	108	3.70	106	83.9	98.3

Sub, subject; Gen, gender; Hgt, height; Wgt, body weight; Iwgt, ideal body weight; V_{air}, airway volume defined by subject age (yr) plus ideal body weight in lb. (29); FVC, forced vital capacity; FEV_1, forced expiratory volume in 1 s; %pred, % predicted; FEV_1/FVC, normalized forced expiratory volume in 1 s by forced vital capacity.

The Institutional Review Board at the University of California, Irvine approved the protocol, and written, informed consent was obtained from all subjects.

Protocol. Each subject performed two types of exhalation maneuvers in both air and heliox. When air is replaced with heliox as the insufflating gas, the molecular diffusivity, $D_{NO,i}$, of NO and gas density change significantly. $D_{NO,i}$ increases by ~2.3-fold (i.e., $D_{NO,heliox} \approx 2.3\ D_{NO,air}$) (14), and gas density decreases by approximately threefold (12). The former enhances gas-phase diffusion of NO (the impact is primarily in the small airways and is the desired effect for this study), whereas the latter reduces mixing and axial dispersion of NO primarily in the larger airways, which has a negligible impact on this study (see DISCUSSION for details).

The first maneuver was three repetitions of a single-breath maneuver that included a preexpiratory 20-s breath hold followed by a decreasing flow rate (from ~6 to ~1% of vital capacity per second) (29) to measure C_{NOpeak}, W_{50}, $V_{I,II}$, and $A_{I,II}$, and to estimate several flow-independent NO-exchange parameters. A positive pressure of >5 cmH_2O was maintained to prevent nasal contamination during the breath hold (1). A Starling resistor (Hans Rudolph, Kansas City, MO) with a variable resistance was used to progressively decrease the flow rate during the exhalation. A schematic of the experimental apparatus has been previously presented (29). The second maneuver was a vital capacity maneuver performed in triplicate to collect plateau NO concentration on the basis of the American Thoracic Society guidelines (1) in which the exhalation flow rate was maintained at a target of 50 ml/s.

Before performing the breathing maneuvers in heliox, each subject inhaled heliox during quiet tidal breathing for 2 min to washout nitrogen in the functional residual capacity. To determine the potential impact of nitrogen in the residual volume, each subject also performed the preexpiratory breath hold maneuver with a 20-s breath hold in the presence of heliox without tidal breathing heliox before the maneuver. After measurement of the indexes of NO-exchange dynamics (4, 5, 25), general spirometry such as FVC, FEV_1, and FEV_1 by FVC were measured in all subjects (Vmax229; Sensormedics, Yorba Linda, CA) by using the best performance (see Table 1) from three consecutive maneuvers.

Airstream analysis. A chemiluminescence NO analyzer (NOA280, Sievers, Boulder, CO) was used to measure the exhaled NO concentration. The instrument was calibrated on a daily basis by using a certified NO gas (45 ppm NO in 100% N_2 for air calibration and 45 ppm NO in 100% He for heliox calibration; Sievers). The zero-point calibration was performed with a NO filter (Sievers) immediately before the collection of a profile. Calibration with 80% of carrier gas (either nitrogen or helium as in the case of air or heliox, respectively) balanced with oxygen resulted in a negligible change in the response of the instrument (<2% for helium). The flow rate and pressure signals were measured via a pneumotachometer (RSS100, Hans Rudolph). The pneumotachometer was calibrated daily, set to provide the flow in units of STPD, and accounted for changes in gas properties (e.g., viscosity) when using heliox.

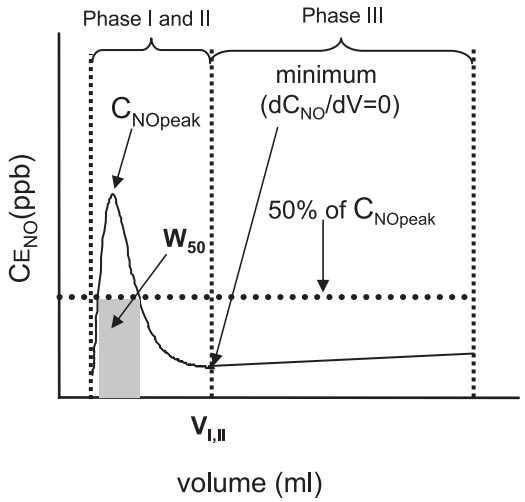

Fig. 1. Definitions of C_{NOpeak}, W_{50}, $V_{I,II}$, and $A_{I,II}$ are presented in a schematic of a representative exhalation nitric oxide (NO) profile using the single-breath technique with a preexpiratory breath hold and a decreasing exhalation flow rate. The distinction between phases I and II and phase III is the point of zero slope (minimum point) in the exhalation profile, as previously described (28). All parameters are defined in the *Glossary*.

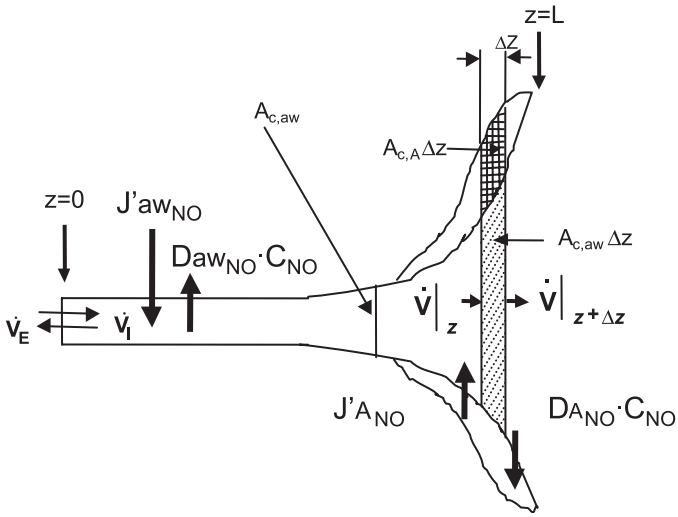

Fig. 2. Schematic of the trumpet model based on the symmetric bifurcating structure and anatomic data of Weibel (32). The values of *z* at the start and end of the trumpet are defined during inspiration. These values switch during expiration (see text for details). All parameters are defined in the *Glossary*.

Empirical data analysis. Experimental single-exhalation profiles with preexpiratory breath hold were characterized empirically by C_{NOpeak}, W_{50}, total $V_{I,II}$, defined as the minimum point (zero slope or $dCE_{NO}/dV = 0$) in the exhalation profile (29), and $A_{I,II}$ (Fig. 1). In addition, the plateau concentration at a constant flow rate of 50 ml/s ($CE_{NO,50}$), as previously described by the American Thoracic Society (1), was also determined.

Model Development and Simulation

Two-compartment model. A previously described two-compartment model was used to estimate four flow-independent NO exchange parameters: *1*) $J'aw_{NO}$ (pl/s), *2*) Daw_{NO} ($pl \cdot s^{-1} \cdot ppb^{-1}$), *3*) CA_{NO} (ppb), and *4*) mean airway tissue NO concentration, Caw_{NO} (ppb) (equal to the ratio of $J'aw_{NO}$ to Daw_{NO}). A detailed description of the mathematical algorithm to calculate the parameters has been previously described (29).

Trumpet model. The impact of axial diffusion was assessed utilizing a "trumpet model" of the lungs (17) by comparing simulations that included ($D_{NO,air} = 0.23\ cm^2/s$ for air or $D_{NO,heliox} = 0.52\ cm^2/s$ for heliox) and excluded ($D_{NO,air} = 0$) axial diffusion. The structure of the trumpet model (see Fig. 2) is based on Weibel's anatomic data (32) (see APPENDIX for the governing equation and boundary conditions).

Development of a parameter estimation routine is beyond the scope of this work. Hence, mean values of flow-independent parameters from the nine subjects, as determined from the two-compartment model, were utilized in the trumpet model simulations. The parameters were then adjusted to predict two indexes that characterize the single-breath maneuvers (29). These include $A_{I,II}$ and the dynamic shape of phase III. The dynamic shape of phase III is characterized by

the normalized root mean square error between model prediction and experimental data, $\bar{R}_{III}$, defined by

$$\bar{R}_{III} = \sqrt{\sum_{i=1}^{n_{III}} \left[\frac{C^*_{E_{NO}}(i) - \hat{C}_{E_{NO}}(i)}{\hat{C}_{E_{NO}}(i)} \right]^2 \Big/ n_{III}} \quad (1)$$

In this fashion, $\bar{R}_{III}$ is the mean fractional deviation of the model prediction to the experimental data (i.e., the gold standard) in phase III. In a fashion similar to $\bar{R}_{III}$, $A^*_{I,II}$ values are also referenced to an optimal or gold standard determined from experimental data. The new variable is denoted $\bar{A}_{III}$ and is defined as

$$\bar{A}_{I,II} = \frac{|A^*_{I,II} - \hat{A}_{I,II}|}{\hat{A}_{I,II}} \quad (2)$$

where $\hat{A}_{I,II}$ is the area under the curve in phase I and II of the composite experimental profile (Fig. 3). Thus $A_{I,II}$ is interpreted as the fractional deviation from the gold standard (same as $\bar{R}_{III}$).

Statistics. Data were analyzed by a paired *t*-test. All variables were assumed to be normally distributed. All statistical tests were performed on the untransformed data. A P value of <0.05 was considered statistically significant.

RESULTS

Figure 3 presents the composite experimental profile for the single-breath maneuver with a 20-s preexpiratory breath hold with a decreasing exhalation flow rate. The composite profile was attained by taking the mean exhaled concentration at equivalent exhaled volume intervals in the nine healthy subjects. A decrease in the concentration of NO exhaled in all three phases of the single-exhalation breathing maneuver was observed when heliox was the insufflating gas, although C_{NOpeak} was not statistically lower (see Fig. 4 below).

C_{NOpeak}, W_{50}, $V_{I,II}$, and $A_{I,II}$ for all nine subjects are presented in Fig. 4 to demonstrate specific differences in the exhaled NO profile between air and heliox breathing. C_{NOpeak} (Fig. 4*A*) was not impacted by the presence of heliox; however, W_{50}, $V_{I,II}$, and $A_{I,II}$ (Fig. 4, *B–D*) were all significantly reduced (mean values of 26, 23, and 36%, respectively).

There were no differences in C_{NOpeak}, W_{50}, and $V_{I,II}$ with or without 2 min of tidal breathing heliox before the single-exhalation maneuver. Mean (SD) values for C_{NOpeak}, W_{50}, and $V_{I,II}$ in the absence or presence of the 2-min heliox tidal breathing were 52 (20) and 53 (30) ppb, 139 (28) and 124 (27) ml, and 544 (88) and 485 (55) ml, respectively. In addition, mean (SD) values for $C^*_{E_{NO,50}}$ in the absence or presence of the 2-min heliox tidal breathing were 10.8 (5.94) and 11.4 (6.53) ppb, respectively, and were not statistically different. $\hat{A}_{I,II}$ for air and heliox were 12,800 and 8,150 ppb·ml, respectively.

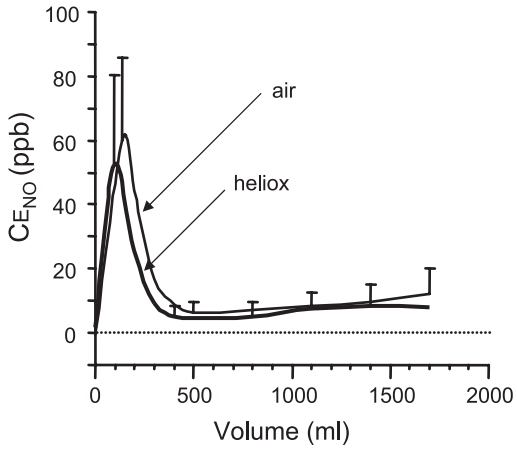

Fig. 3. Composite experimental NO exhalation profile with standard deviation is presented for 20-s breath hold followed by a decreasing exhalation flow rate maneuver for air (solid line) and for heliox (heavy solid line).

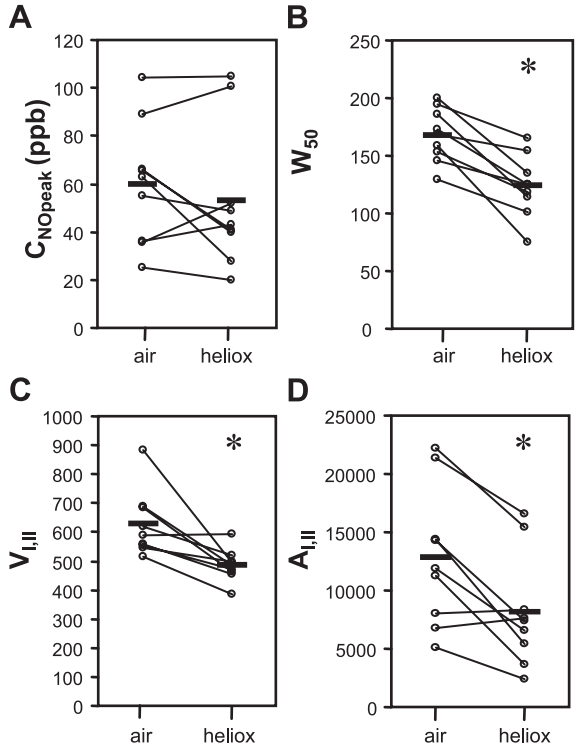

Fig. 4. Four measured parameters are presented for 20-s breath hold followed by a decreasing exhalation flow rate maneuver for air and heliox: C_{NOpeak} (*A*), W_{50} (*B*), $V_{I,II}$ (*C*), and $A_{I,II}$ (*D*). The mean values for air and heliox are shown by the solid dark bar. *Statistical significance between air and heliox (paired *t*-test, $P < 0.05$).

$C_{E_{NO,50}}$ is presented in Table 2 for air and heliox. *Subject 6* could not adequately perform the constant-exhalation flow-rate maneuver for both air and heliox, and *subject 5* could not adequately perform the constant-exhalation flow-rate maneuver in the presence of heliox. Mean $C_{E_{NO,50}}$ was significantly decreased by 45% in the presence of heliox (8.0 ppb compared with 14.6 ppb).

Figure 5 presents the model-simulated exhalation NO profile for the single exhalation with a 20-s preexpiratory breath hold and decreasing exhalation flow rate with either air (*A*) or heliox (*B*) as the insufflating gas. The following mean values for the flow-independent NO parameter values determined from the two-compartment model were utilized: $J'aw_{NO}$ = 734 pl/s, Daw_{NO} = 5.03 pl·s^{-1}·ppb^{-1}, and $C_{A_{NO}}$ = 2.55 ppb for air and $J'aw_{NO}$ = 485 pl/s, Daw_{NO} = 4.24 pl·s^{-1}·ppb^{-1}, and $C_{A_{NO}}$ = 2.36 ppb for heliox. For both cases, $D_{A_{NO}}$ was set to 1,467 pl·s^{-1}·ppb^{-1} (20, 28). (Note that $C_{A_{NO}} = J'_{A_{NO}}/D_{A_{NO}}$.) The following three different cases are shown: *1*) the trumpet model in the absence of axial diffusion, *2*) the trumpet model in the presence of axial diffusion ($D_{NO,air}$ = 0.23 or $D_{NO,heliox}$ = 0.52), and *3*) the trumpet model in the presence of axial diffusion ($D_{NO,air}$ = 0.23 or $D_{NO,heliox}$ = 0.52) when $J'aw_{NO}$ is

Table 2. *Model-predicted and experimental C_{NOplat} at 50 ml/s of subjects*

	$\dot{V}_E$ and $C_{E_{NO,50}}$ (experimental data)			
	Air		Heliox	
Subject	ml/s	ppb	ml/s	ppb
1	*45.8*	*11.8*	*50.9*	*8.03*
2	*51.0*	*10.9*	*50.7*	*7.98*
3	*54.3*	*7.01*	*41.5*	*3.09*
4	*70.3*	*3.06*	*65.3*	*2.82*
5	*64.2*	*33.2*	*NA*	*NA*
6	*NA*	*NA*	*NA*	*NA*
7	*58.4*	*12.2*	*43.5*	*7.65*
8	*59.1*	*17.0*	*48.1*	*12.5*
9	*47.8*	*21.7*	*63.8*	*12.1*
Mean	*56.4*	*14.6*	*61.0*	*8.00**

NA, not able to complete the maneuver. *Statistically different from air (paired *t*-test with $P < 0.05$)

increased ($J'aw_{NO}$ = 1,100 pl/s) and $C_{A_{NO}}$ is set to zero (both at the boundary $z = L^+$ and by setting $J'_{A_{NO}}$ equal to zero because $J'_{A_{NO}}$ is the product of $C_{A_{NO}}$ and $D_{A_{NO}}$; see *Glossary* and APPENDIX).

In the absence of axial diffusion, the trumpet model reproduces both $A_{I,II}$ and the dynamic shape of phase III compared with the two-compartment model (data not shown). The presence of axial diffusion significantly reduces the concentration of NO in all phases of the exhalation profile but does not impact C_{NOpeak} (Fig. 5*A*). The presence of heliox (increasing molecular diffusivity of NO from 0.23 to 0.52 cm^2/s) further reduces the concentration of NO in all phases but does not impact C_{NOpeak} (Fig. 5*B*). For both air and heliox, values for $\bar{A}_{I,II}$ and $\bar{R}_{III}$ significantly deviate from zero and are equal to 0.45 and 0.10 and 0.50 and 0.21, respectively (Fig. 5, *C* and *D*).

Increasing $J'aw_{NO}$ increases the concentration of NO in all phases of the exhalation profile and thus impacts $A_{I,II}$ and R_{III}. Increasing $J'aw_{NO}$ by 1.5-fold ($J'aw_{NO}$ = 1,100 pl/s) in the presence of axial diffusion ($D_{NO,air}$ = 0.23 cm^2/s), holding Daw_{NO} and $D_{A_{NO}}$ constant (5.03 and 1,467 $pl \cdot s^{-1} \cdot ppb^{-1}$, respectively), and decreasing the alveolar concentration to zero ($C_{A_{NO}} = 0$ and $J'_{A_{NO}} = 0$) provides the optimal simulation ($\bar{A}_{I,II}$ and $\bar{R}_{III}$, improve to 0.25 and 0.04, respectively; see Fig. 5*C*). When this same set of flow-independent parameters is used to simulate heliox ($D_{NO,heliox}$ = 0.52 cm^2/s), the trumpet model is able to simulate phase I and II very accurately ($A_{I,II}$ improves from 0.50 to 0.03), but the impact on phase III is negligible ($\bar{R}_{III}$ is unchanged from 0.21).

DISCUSSION

This is the first study to probe the impact of axial diffusion on NO exchange dynamics in the lungs experimentally by

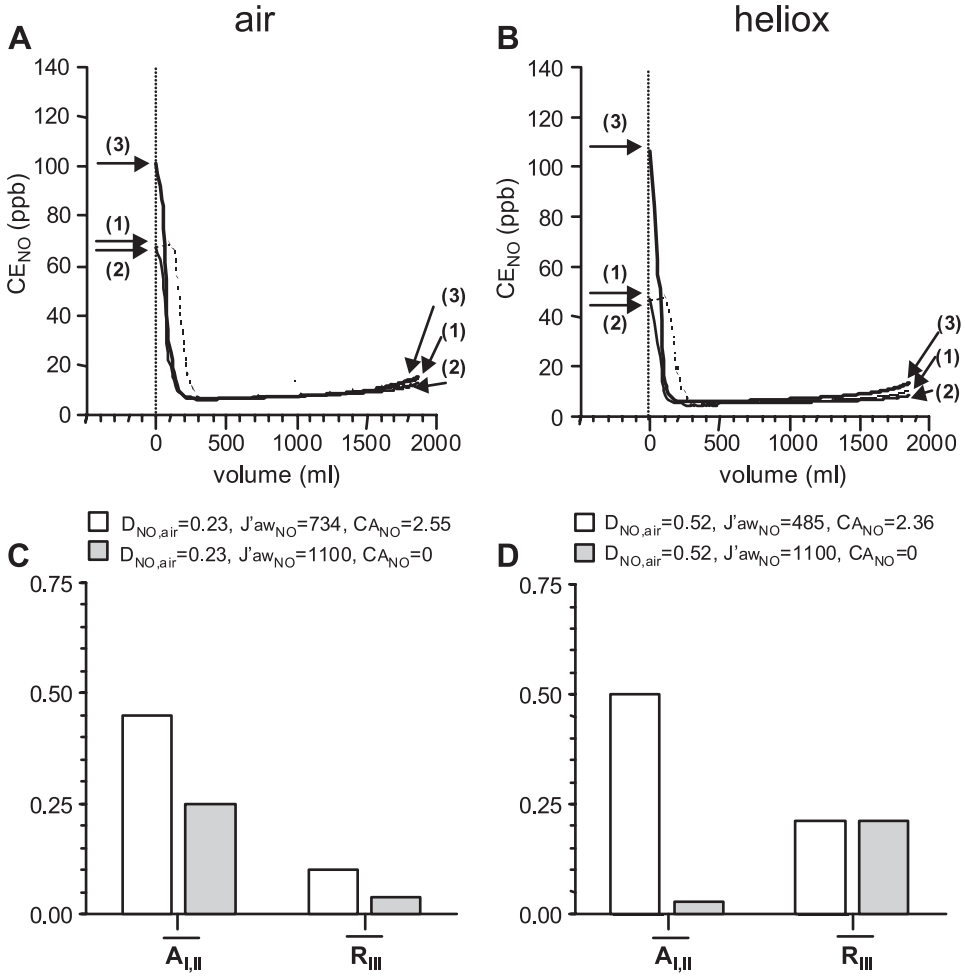

Fig. 5. Model-simulated NO exhalation profiles for air breathing (*A*) and heliox breathing (*B*) from a 20-s breath hold followed by a decreasing flow rate maneuver are presented for 3 different cases: *1*) the trumpet model in the absence of axial diffusion, *2*) the trumpet model in the presence of axial diffusion, and *3*) the trumpet model prediction in the presence of axial diffusion when $J'aw_{NO}$ is increased by 1.5-fold ($J'aw_{NO}$ = 1,100 pl/s) and $C_{A_{NO}}$ = 0 ppb. The following mean values for the flow-independent NO parameter values determined from the 2-compartment model were utilized: $J'aw_{NO}$ = 734 pl/s; Daw_{NO} = 5.03 $pl \cdot s^{-1} \cdot ppb^{-1}$; and $C_{A_{NO}}$ = 2.55 ppb for air and $J'aw_{NO}$ = 485 pl/s; Daw_{NO} = 4.24 $pl \cdot s^{-1} \cdot ppb^{-1}$; and $C_{A_{NO}}$ = 2.36 ppb for heliox. For both cases, $D_{A_{NO}}$ was set to 1,467 $pl \cdot s^{-1} \cdot ppb^{-1}$. (Note that $C_A = J'_{A_{NO}}/D_{A_{NO}}$.) The performance of the model in the presence and absence of axial diffusion is assessed with two indexes ($\bar{A}_{I,II}$ and R_{III}, see text for details) for air (*C*) and heliox breathing (*D*).

manipulating the rate of axial diffusion in the airways with heliox as the insufflating gas. Our results demonstrate that the exhaled NO concentration when heliox is the insufflating gas is decreased in all three phases of the single-exhalation breathing maneuver with a preexpiratory breath hold as well as the $C_{E_{NO,50}}$. In addition, W_{50} of the exhalation profile, $V_{I,II}$, and $A_{I,II}$ after a breath hold are substantially reduced. These experimental observations in the presence of heliox are consistent with a reduced amount of NO eliminated in the exhalation breath and result in a 34% decrease in the estimate for $J'aw_{NO}$ according to a two-compartment model that neglects axial diffusion. When axial diffusion is considered in an alternate model (trumpet model), optimal parameter values predict a 50% increase in $J'aw_{NO}$ and a near-zero $C_{A_{NO}}$ and $J'_{A_{NO}}$.

Impact of Heliox as the Insufflating Gas

NO in the airways is transported by both molecular diffusion (resulting from concentration gradients and random motion of individual NO molecules) and convection (resulting from bulk flow of the insufflating gas). With bulk flow only in the axial direction (i.e., in the absence of mixing), NO transport may be characterized in terms of the Peclet number, Pe, a dimensionless index. Pe corresponds to the ratio of NO mass transport rate by convection (bulk flow) to that by molecular diffusion. Furthermore, Pe is inversely proportional to the molecular diffusivity of NO in the gas phase, $D_{NO,i}$ (i denotes the insufflating gas, either air or heliox) and directly proportional to the product of bulk gas velocity and a characteristic length (usually selected as the airway diameter). The importance of molecular diffusion, relative to convection, increases with decreasing Pe and increasing $D_{NO,i}$.

At high bulk gas velocities (typical of the larger airways), fluid mixing at airway bifurcations (called axial dispersion) also impacts NO transport rates. Previous work (3, 16, 26) demonstrates that axial dispersion is dependent on flow rate, geometry, and the fluid's physical properties, with mathematical characteristics similar to molecular diffusion. Scherer et al. (16) and others (3, 26) have described the combined effects of molecular diffusion and axial dispersion in terms of an effective diffusivity, $D^*_{NO,i}$. These experiments used nitrogen (with similar physical properties to air) as the insufflating gas. From these data, $D^*_{NO,i}$ was correlated as the sum of $D_{NO,i}$ and an axial dispersion term, to account for molecular diffusion and gas mixing at airway bifurcations, respectively. The axial dispersion term was proportional to the product of gas velocity and airway diameter. When air is the insufflating gas, the similarity of air and nitrogen allows axial dispersion's impact to be approximated for an airway branch with known gas velocity and diameter.

When Pe is large (e.g., >10), convection dominates NO transport, relative to molecular diffusion, but axial dispersion retains some influence. For heliox, the precise impact of axial dispersion under these conditions remains unclear. Reynolds number, Re, is a dimensionless index, directly proportional to gas density, and for a specific insufflating gas, Re is also proportional to Pe. Because the data of Scherer et al. and others (3, 16, 26) imply that the relative importance of axial dispersion increases with Re, a gas with lower density will have lower Re and will exhibit less mixing. Therefore, the impact of axial dispersion is expected to be less important for heliox than for air at large Pe. Conversely, when Pe is small (e.g., <0.1) molecular diffusion dominates over both convection and axial dispersion.

At typical exhalation flow rates (e.g., 250 ml/s), the precise impact of replacing air with heliox as the insufflating gas in the larger airways (i.e., generation <5) requires further investigation. However, in the smaller airways, convection and gas mixing are much less important and molecular diffusion dominates. Hence, replacing air with heliox significantly enhances molecular diffusion in the smaller airways and provides a means to study the impact of axial diffusion of NO in the lungs.

Impact of Axial Diffusion on Exhaled NO Concentration

When heliox was used as the insufflating gas in the present study, exhaled NO concentration was decreased in breathing maneuvers spanning a range of static and dynamically changing flow rates. This result is consistent with previous (17) and present simulations (Fig. 5) of a trumpet model that considers axial diffusion and is due to diffusion of NO down the concentration gradient (i.e., from high to low concentration) from the airway to the alveolar region.

The presence of heliox did not impact C_{NOpeak} but reduced W_{50}, $V_{I,II}$, and $A_{I,II}$. These findings were confirmed by the trumpet model simulations. The reduced $A_{I,II}$ is due to the reduced W_{50} (thinner peak causes a small area). The reduced W_{50} and $V_{I,II}$ are due to depletion of NO in the smaller airways while a constant C_{NOpeak} is maintained (see Fig. 1, which describes how W_{50} and $V_{I,II}$ are determined). The depletion of NO is a direct result of enhanced axial diffusion of NO from the airways to the alveolar region. The constant C_{NOpeak} is due to a minimal impact of axial diffusion in the larger airways during breath hold. C_{NOpeak} occurs in the first part of the exhaled breath, which is the largest distance from the sink (i.e., the alveolar region) because of axial diffusion. If breath hold time were increased such that a new steady state was achieved in the airway compartment, a lower C_{NOpeak} should be observed. We confirmed this by simulating a 1-h breath hold time using the trumpet model, and C_{NOpeak} decreased by 2% (146 ppb, the ratio of $J'aw_{NO}/Daw_{NO}$ or Caw_{NO}, to 143 ppb). Thus concentrations of NO throughout the airway tree during a breath hold are potentially impacted; however, for breath hold times less than ~1 min, the impact is only observed in the small airways.

Impact of Axial Diffusion on Flow-Independent NO Parameters

Previous results from our group and others (17, 31), as well as simulations in the present study (Fig. 5), demonstrate that axial diffusion results in a loss of NO produced in the airways to the alveolar region. The result is a decrease in the estimated source of NO from the airways (i.e., $J'aw_{NO}$). This hypothesis is confirmed by the 34% reduction in $J'aw_{NO}$ (735 pl/s compared with 485 pl/s) predicted by the two-compartment model, which neglects axial diffusion when heliox replaces air as the insufflating gas and rate of the axial diffusion is increased by 2.3-fold. Thus, to simulate the exhaled concentration observed experimentally with a model that considers axial diffusion, the endogenous source of NO in the airways (i.e., $J'aw_{NO}$) needs to be increased. The present study suggests that 1.5-fold increase (50%) of $J'aw_{NO}$ in the presence of air (from 735 to

1,100 pl/s) and a 2.3-fold increase (130%) in the presence of heliox (485 to 1,100 pl/s) combined with a zero alveolar concentration and source (decrease in $C_{A_{NO}}$ from ~2.5 ppb to 0, and $J'_{A_{NO}} = 0$) is necessary to compensate for the effects of axial diffusion in all three phases of the exhalation profile (Fig. 5).

Of note is the observation that the simulation indexes (i.e., R_{III}) for heliox are poorer than air. This is likely due to remaining simplifications of the trumpet model that are exaggerated by the differences between heliox and air. For example, the trumpet model assumes that $J'aw_{NO}$ is constant per unit airway volume (resulting in a decrease in $J'aw_{NO}$ per unit surface area). This model structure is consistent with reports that the lower airways do not produce as much NO as the larger airways (22) but may not represent the precise distribution. Using the optimal parameter values ($J'aw_{NO}$ = 1,100 pl/s and $C_{A_{NO}}$ = 0 ppb) and a constant exhalation flow rate of 50 ml/s, the trumpet model predicts the concentration in generation 2 (z = 18.7 cm) to be 10.9 ppb, which is 71% of the exhaled concentration at the mouth (z = 0, 15.4 ppb). Although somewhat higher, this value is comparable to Silkoff et al. (22), who reported that ~50% of exhaled NO arises from the upper airways (generations 0–2). If a greater or smaller flux of NO is present in the airways than our model structure, then a greater or smaller, respectively, contribution of axial diffusion on exhaled NO is simulated, which introduces error in the relative impact of axial diffusion. In addition, as mentioned by Van Muylem et al. (31), other factors such as asymmetry of the airway tree and inhomogeneous ventilation may affect the exhalation profile of NO and would differentially impact the simulation of heliox compared with air because of differences in density between the two gases.

Finally, it is important to emphasize that our trumpet model structure limits the simulations of alveolar concentration to a fixed steady-state value. Hence, we cannot rule out the possibility that, even in the presence of a zero alveolar source, the alveolar concentration may be nonzero because of backdiffusion of NO from the airways. This simulation requires a more advanced model in which a separate mass balance on an alveolar compartment is coupled to the mass balance in the airway compartment.

The prediction of a zero or near-zero alveolar concentration in the presence of a zero alveolar source suggests the possibility that previous reports of $C_{A_{NO}}$ values that range from 1 to 5 ppb (7, 10, 18, 19, 20) may represent NO in or near the alveolar and respiratory bronchiole region, but the source may be the airways because of backdiffusion. The most commonly used technique to estimate $C_{A_{NO}}$ is a plot of $\dot{V}_{NO}$ vs. $\dot{V}_E$ (30). For exhalation flow rates >50 ml/s in adults, the slope of this plot is an estimate of $C_{A_{NO}}$ and the intercept an estimate of $J'aw_{NO}$. We hypothesized that even if $C_{A_{NO}}$ were zero, this plot would predict a positive slope (i.e., a nonzero $C_{A_{NO}}$) because the impact of axial diffusion (and thus loss of NO to the alveolar region) would be reduced as the exhalation flow rate increased. To test this hypothesis and to determine the magnitude of this phenomenon, the trumpet model was used to predict $C_{ENO,i}$ (and thus $\dot{V}_{NO}$) at five different $\dot{V}_E$ values (50, 100, 150, 200, 300, and 500 ml/s) by using the optimal set of flow-independent NO parameters ($J'aw_{NO}$ = 1,100 pl/s, Daw_{NO} = 5.03 $pl \cdot s^{-1} \cdot ppb^{-1}$, and $C_{A_{NO}}$ = 0 ppb) in the presence and absence of axial diffusion.

Figure 6 demonstrates the trend in the slope and intercept of $\dot{V}_{NO}$ vs. $\dot{V}_E$ in the absence (Fig. 6*A*) and presence (Fig. 6*B*) of axial diffusion for different subgroups of the five exhalation flow rates (three of the five flow rates, i.e., 50, 100, and 150 ml/s). In the absence of axial diffusion (equivalent to the two-compartment model) with $C_{A_{NO}}$ = 0, the predicted slope is slightly positive (0.36 ppb) when the three lowest flow rates are used and then approaches zero as higher flow rates are used. The slightly positive value at lower flow rates as well as the slight nonlinear relationship (i.e., $r^2 < 1.0$) is due to the fact that, as the flow rate decreases, the airway compartment concentration increases (because of a longer residence time of air in the compartment) and the airway flux decreases slightly ($Jaw_{NO} = J'aw_{NO} - Daw_{NO} \times C_{NO}$) as previously described (29). In the presence of axial diffusion with $C_{A_{NO}}$ = 0, the slope is 2.1 ppb for a flow rate range of 50–150 ml/s and decreases to 0.4 ppb over the flow rate range of 200–500 ml/s. This value for the slope (0.4–2.1 ppb) is consistent with

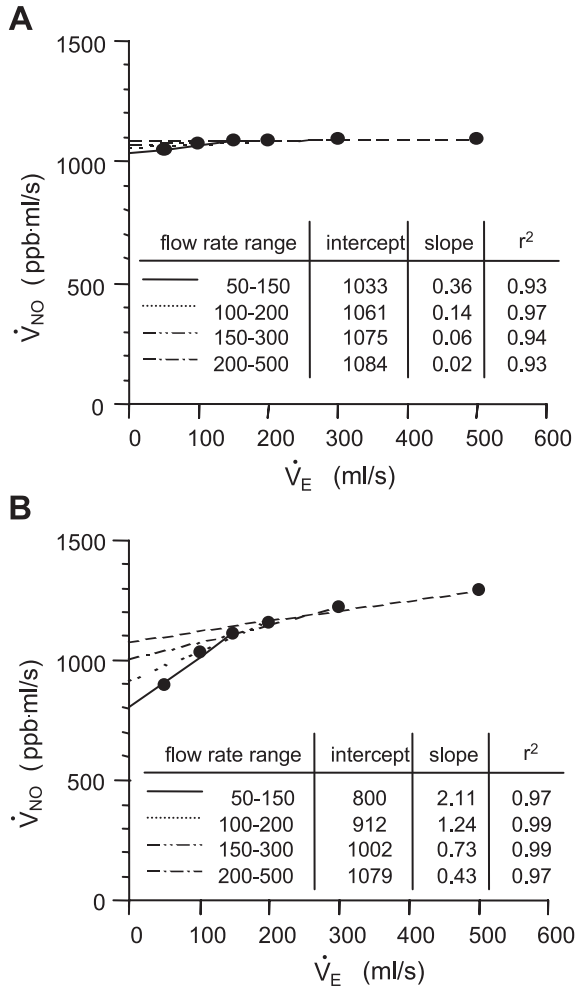

Fig. 6. Elimination rate of NO is plotted vs. the exhalation flow rate as predicted in the absence (*A*) and presence (*B*) of axial diffusion. In all simulations, the optimal values for the flow-independent NO exchange parameters ($J'aw_{NO}$ = 1,100 pl/s and $C_{A_{NO}}$ = 0 ppb) were used to simulate plateau concentration at a constant flow rate of 50 ml/s ($C_{ENO,50}$) and thus the elimination rate. Linear regression is performed through a sequence of 3 consecutive data points, and the intercept, which has been previously interpreted as $J'aw_{NO}$, and the slope, which has been previously interpreted as $C_{A_{NO}}$, are presented according to 4 different flow rate ranges.

reported $C_{A_{NO}}$ determined by using the slope of the relationship $\dot{V}_{NO}$ vs. $\dot{V}_E$ using the two-compartment model, which neglects axial diffusion (7, 10, 18–20). Thus $C_{A_{NO}}$ may be near zero for healthy adults, and the reported 1- to 3-ppb range determined from the slope of $\dot{V}_{NO}$ vs. $\dot{V}_E$ (7, 10, 18–20) may be an artifact from neglecting axial diffusion.

In conclusion, in the presence of axial diffusion, the trumpet model predicts a significant backdiffusion of NO from the airways into the alveolar region, which is demonstrated experimentally by using heliox as the insufflating gas. Backdiffusion of NO from the airways to the alveolar region results in a significant loss of NO, which does not appear in the exhaled breath. Thus models that neglect axial diffusion underestimate the maximum airway flux by as much as 50%, and the alveolar concentration reported in healthy adults may reflect, in part, NO produced in the small airways. We conclude that accurate estimation of flow-independent NO exchange parameters, and thus partitioning of exhaled NO into airway and alveolar contributions, must include mathematical models that consider axial diffusion of NO in the gas phase. In addition, future studies must quantify the impact of axial diffusion for subjects with key inflammatory diseases of the airways such as asthma or cystic fibrosis, as well as diseases that involve inflammation of the alveolar region.

APPENDIX

Governing Equation

The governing partial differential equation for C_{NO} (ppb) is obtained from a mass balance over a differential volume of length Δz:

$$\left\{A_{c,aw} + \left[\frac{N(z)}{N_t}\right]A_{c,A}\right\}\frac{dC_{NO}}{dt} = -\dot{V}\frac{dC_{NO}}{dz} + D_{NO,air}\frac{d}{dz}\left[A_{c,aw}(z)\frac{dC_{NO}}{dz}\right] + (\tilde{J}'aw_{NO} - \tilde{D}aw_{NO}C_{NO})\left[1 - \frac{N(z)}{N_{max}}\right] + (\tilde{J}'_{A_{NO}} - \tilde{D}_{A_{NO}}C_{NO})\left[\frac{N(z)}{N_t}\right] \quad (A1)$$

where $N(z) = 0$ for $z < 26.8$ cm, $N_{max} = 143 \times 10^6$, and N_t is total number of alveoli in Weibel lung (298.1×10^6).

Initial and Boundary Conditions

The initial condition for *Eq. A1* for inspiration is $C_{NO}(z,t = 0) = 0$, and for expiration it is equal to the concentration profile just before exhalation (either after the 20-s breath hold for *breathing maneuver 1* or end-inspiration for *breathing maneuver 2*). The boundary conditions for *Eq. 1* are as follows:

$$\text{Inspiration:}\quad C_{NO}(z = 0^-,t) = 0 \quad \text{(ambient air zero concentration)} \quad (A2)$$

$$C_{NO}(z = L^+,t) = C_{A_{NO}} \quad (A3)$$

$$\text{Expiration:}\quad C_{NO}(z = 0^-,t) = C_{A_{NO}} \quad (A4)$$

$$\frac{dC_{NO}(z = L,t)}{dz} = 0 \quad \text{(no flux at end of airway)} \quad (A5)$$

where $z = 0^-$ refers to a single numerical node (i.e., z position) just before the start of the trumpet and t is time. The boundaries are reversed for expiration (i.e., $z = 0^-$ is always the position where air enters the trumpet). The node just beyond the end of the trumpet is expressed as $C_{A_{NO}}$, which represents a fixed steady-state alveolar concentration, specifically, 2.55 ppb or 0 ppb in the present simulations.

ACKNOWLEDGMENTS

We thank the General Clinical Research Center (GCRC) at University of California, Irvine.

GRANTS

This work was supported by grants from the National Institutes of Health (HL-070645, HD-26939, RR-00827).

REFERENCES

1. **American Thoracic Society.** Recommendations for standardized procedures for the online and offline measurement of exhaled lower respiratory nitric oxide and nasal nitric oxide in adults and children—1999. *Am J Respir Crit Care Med* 160: 2104–2117, 1999.
2. **Barnes PJ and Kharitonov SA.** Exhaled nitric oxide: a new lung function test. *Thorax* 51: 233–237, 1996.
3. **Chatwin P.** On the longitudinal dispersion of passive contaminant in oscillatory flows in tubes. *J Fluid Mech* 71: 513–527, 1975.
4. **Deykin A, Halpern O, Massaro AF, Drazen JM, and Israel E.** Expired nitric oxide after bronchoprovocation and repeated spirometry in patients with asthma. *Am J Respir Crit Care Med* 157: 769–775, 1998.
5. **Deykin A, Massaro AF, Coulston E, Drazen JM, and Israel E.** Exhaled nitric oxide following repeated spirometry or repeated plethysmography in healthy individuals. *Am J Respir Crit Care Med* 161: 1237–1240, 2000.
6. **DuBois AB, Kelley PM, Douglas JS, and Mohsenin V.** Nitric oxide production and absorption in trachea, bronchi, bronchioles, and respiratory bronchioles of humans. *J Appl Physiol* 86: 159–167, 1999.
7. **Hogman M, Drca N, Ehrstedt C, and Merilainen P.** Exhaled nitric oxide partitioned into alveolar, lower airways and nasal contributions. *Respir Med* 94: 985–991, 2000.
8. **Hyde RW, Geigel EJ, Olszowka AJ, Krasney JA, Forster RE 2nd, Utell MJ, and Frampton MW.** Determination of production of nitric oxide by lower airways of humans—theory. *J Appl Physiol* 82: 1290–1296, 1997.
9. **Lehtimaki L, Kankaanranta H, Saarelainen S, Hahtola P, Jarvenpaa R, Koivula T, Turjanmaa V, and Moilanen E.** Extended exhaled NO measurement differentiates between alveolar and bronchial inflammation. *Am J Respir Crit Care Med* 163: 1557–1561, 2001.
10. **Lehtimaki L, Kankaanranta H, Saarelainen S, Turjanmaa V, and Moilanen E.** Inhaled fluticasone decreases bronchial but not alveolar nitric oxide output in asthma. *Eur Respir J* 18: 635–639, 2001.
11. **Lehtimaki L, Turjanmaa V, Kankaanranta H, Saarelainen S, Hahtola P, and Moilanen E.** Increased bronchial nitric oxide production in patients with asthma measured with a novel method of different exhalation flow rates. *Ann Med* 32: 417–423, 2000.
12. **Papamoschou D.** Theoretical validation of the respiratory benefits of helium-oxygen mixtures. *Respir Physiol* 99: 183–190, 1995.
13. **Pietropaoli AP, Perillo IB, Torres A, Perkins PT, Frasier LM, Utell MJ, Frampton MW, and Hyde RW.** Simultaneous measurement of nitric oxide production by conducting and alveolar airways of humans. *J Appl Physiol* 87: 1532–1542, 1999.
14. **Reid RC, Prausnitz JM, and Poling BE.** *The Properties of Gases and Liquids*. New York: McGraw-Hill, 1988.
15. **Schedin U, Frostell C, Persson MG, Jakobsson J, Andersson G, and Gustafsson LE.** Contribution from upper and lower airways to exhaled endogenous nitric oxide in humans. *Acta Anaesthesiol Scand* 39: 327–332, 1995.
16. **Scherer PW, Shendalman LH, Greene NM, and Bouhuys A.** Measurement of axial diffusivities in a model of the bronchial airways. *J Appl Physiol* 38: 719–723, 1975.
17. **Shin HW and George SC.** Impact of axial diffusion on nitric oxide exchange in the lungs. *J Appl Physiol* 93: 2070–2080, 2002.
18. **Shin HW, Rose-Gottron CM, Cooper DM, Hill M, and George SC.** Impact of high-intensity exercise on nitric oxide exchange in healthy adults. *Med Sci Sports Exerc* 35: 995–1003, 2003.

19. **Shin HW, Rose-Gottron CM, Cooper DM, Newcomb RL, and George SC.** Airway diffusing capacity of nitric oxide and steroid therapy in asthma. *J Appl Physiol* 96: 65–75, 2004.
20. **Shin HW, Rose-Gottron CM, Perez F, Cooper DM, Wilson AF, and George SC.** Flow-independent nitric oxide exchange parameters in healthy adults. *J Appl Physiol* 91: 2173–2181, 2001.
21. **Shin HW, Rose-Gottron CM, Sufi RS, Perez F, Cooper DM, Wilson AF, and George SC.** Flow-independent nitric oxide exchange parameters in cystic fibrosis. *Am J Respir Crit Care Med* 165: 349–357, 2002.
22. **Silkoff PE, McClean PA, Caramori M, Slutsky AS, and Zamel N.** A significant proportion of exhaled nitric oxide arises in large airways in normal subjects. *Respir Physiol* 113: 33–38, 1998.
23. **Silkoff PE, McClean PA, Slutsky AS, Furlott HG, Hoffstein E, Wakita S, Chapman KR, Szalai JP, and Zamel N.** Marked flow-dependence of exhaled nitric oxide using a new technique to exclude nasal nitric oxide. *Am J Respir Crit Care Med* 155: 260–267, 1997.
24. **Silkoff PE, Sylvester JT, Zamel N, and Permutt S.** Airway nitric oxide diffusion in asthma: role in pulmonary function and bronchial responsiveness. *Am J Respir Crit Care Med* 161: 1218–1228, 2000.
25. **Silkoff PE, Wakita S, Chatkin J, Ansarin K, Gutierrez C, Caramori M, McClean P, Slutsky AS, Zamel N, and Chapman KR.** Exhaled nitric oxide after β2-agonist inhalation and spirometry in asthma. *Am J Respir Crit Care Med* 159: 940–944, 1999.
26. **Taylor G.** Dispersion of soluble matter in solvent flowing slowly through a tube. *Proc R Soc Lond B Biol Sci* 219: 186–203, 1953.
27. **Tsoukias NM and George SC.** A two-compartment model of pulmonary nitric oxide exchange dynamics. *J Appl Physiol* 85: 653–666, 1998.
28. **Tsoukias NM and George SC.** Impact of volume-dependent alveolar diffusing capacity on exhaled nitric oxide concentration. *Ann Biomed Eng* 29: 731–739, 2001.
29. **Tsoukias NM, Shin HW, Wilson AF, and George SC.** A single-breath technique with variable flow rate to characterize nitric oxide exchange dynamics in the lungs. *J Appl Physiol* 91: 477–487, 2001.
30. **Tsoukias NM, Tannous Z, Wilson AF, and George SC.** Single-exhalation profiles of NO and CO_2 in humans: effect of dynamically changing flow rate. *J Appl Physiol* 85: 642–652, 1998.
31. **Van Muylem A, Noel C, and Paiva M.** Modeling of impact of gas molecular diffusion on nitric oxide expired profile. *J Appl Physiol* 94: 119–127, 2003.
32. **Weibel ER.** *Morphometry of the Human Lung*. Berlin: Springer-Verlag, 1963.